Hans-Christian MOEHRING[1], Dina BECKER[1*],
Clemens MAUCHER[1], Rocco EISSELER[1],
Jonas RINGGER[1]

INFLUENCE OF THE SUPPORT STRUCTURE ON THE BANDSAWING PROCESS WHEN SEPARATING LPBF COMPONENTS FROM THE BUILDING PLATFORM

The method of laser powder bed fusion (LPBF) is an additive manufacturing process and allows great freedom of component geometry due to the layer-by-layer structure. The LPBF components are printed on a substrate plate and must be separated from the plate afterwards. Support structures are used to attach LPBF components to the substrate plate and to sustain overhanging parts. The cutting of the components is mainly carried out by means of a sawing process using the support structure. The forces occurring during this process are very challenging because the component has to be cut off without damage or deformation. The present study investigates and discusses the resultant forces and vibrations during the sawing of LPBF components made of titanium alloy Ti6Al4V using two different support structures. The components were arranged on the substrate plate at angles of 0°, 5°, 10°, 15°, 45° and 90° to the direction of primary motion.

1. INTRODUCTION

In times of raw material shortages, unstable markets and the growing importance of resource-saving production, additive manufacturing is increasingly coming to the fore [1]. In contrast to established manufacturing processes, additive manufacturing enables an almost infinite freedom of designable geometries due to the layer-by-layer structure of a component [2]. This enables an increase in the functional integration of components as well as their load-oriented weight optimization [3, 4]. The method of laser powder bed fusion (LPBF) is one of the most important additive manufacturing processes to produce metallic components made of metal powders [5, 6]. The powder is fused into individual layers with the help of a laser beam. Various steels, aluminium, titanium and numerous alloys are suitable as basic materials for this process.

Many industrial applications require the use of complex, thin-walled components, especially ones with internal, complex channels for coolants or lubricants. The method of LPBF is particularly suitable to produce such components. Thin-walled structures can be

varied by the energy applied and the focus diameter of the laser. Kranz et al. [7] recommended a minimum wall thickness of 0.3 mm for LPBF components made of titanium alloy.

The components put up on a substrate plate. Support structures are provided as connecting elements between the substrate plate and the components. After the printing process, the components must be separated from the substrate plate. For that purpose, sawing processes can be used, which are becoming increasingly popular in this area due to their cost effectiveness. In order not to damage the components during cutting and to keep the effort for reprocessing the substrate plate as low as possible, the aim is to carry out the saw cut only in the area of the support structures and as close as possible to the surface of the substrate plate.

According to studies by Bhuvanesh and Sathiya [8] as well as Isaev et al [9], especially thin-walled components can start to vibrate when the teeth act on the delicate support structures during the sawing process. This can affect the geometrical accuracy of the components so that they may even break in the extreme case. To counter this problem, supporting clamping systems can be used which are adapted to the individual component contour. In earlier studies by the authors, additively manufactured clamping jaws for the sawing of thin-walled LPBF components were already developed and successfully tested [10].

An alternative approach is to increase the process stability during the separation by means of adapted support structures. The very dynamic machining forces during sawing can be strongly influenced by the design and distribution of the individual support structure elements. Among other things, Denkena et al. investigated the feed force when milling additively manufactured components made of Inconel 718. When support structures with a high degree of perforation in the outer contour were used, the feed force was significantly lower than for support structures with a comparatively low degree of perforation [11]. Hintze et al. described a great influence of the support structure design on the operation process during milling [12]. They found a strong correlation between the material volume fraction and the process forces during milling. Maucher et al. also examined this interaction during the drilling process. The disadvantageous effects of the support structures on the machining process were shown here as well. Based on these findings, Maucher et al. proposed adapted support structure geometries [13] as well as adapted process parameters to selectively weaken the material in order to improve the machining process [14].

Although the separation of component and substrate plate by means of sawing has become a common intermediate step in the additive subtractive LPBF process chain, there is still comparatively little knowledge about the operation process in this special form of sawing. For this reason, the presented study investigated and discussed the separation of LPBF test components made of Ti6Al4V titanium alloy powder from a substrate plate. The investigations were focussed on the influence of the design and the positioning of the support structure on the machining forces and vibrations during bandsawing.

2. DESCRIPTION OF THE LPBF COMPONENT

For the investigations of the sawing process, test components were prepared using the method of laser powder bed fusion (LPBF). For this purpose, a total of seven cubes with

the same dimensions of 10 mm × 7 mm × 3 mm were distributed on a circular substrate plate with a diameter of $d = 100$ mm. A linearly arranged support structure was selected for six of the cubes (Fig. 1a top). The support structure of the seventh cube was designed in the form of a grid (Fig. 1a bottom). Figure 1b shows the distribution and orientation of the individual cubes on the substrate plate. The material volume of the linearly arranged support structure was $V_l = 99$ mm³, whereas that of the grid-shaped support structure was $V_g = 198$ mm³.
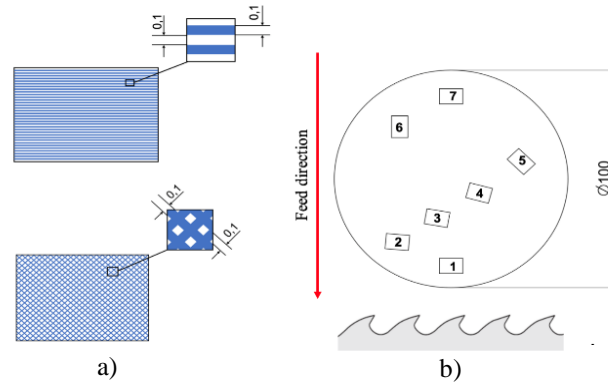

Fig. 1. Cubes with a linearly arranged support structure (top) and a grid-shaped support structure (bottom) as well as substrate plate with distribution and orientation of the individual cubes (b)
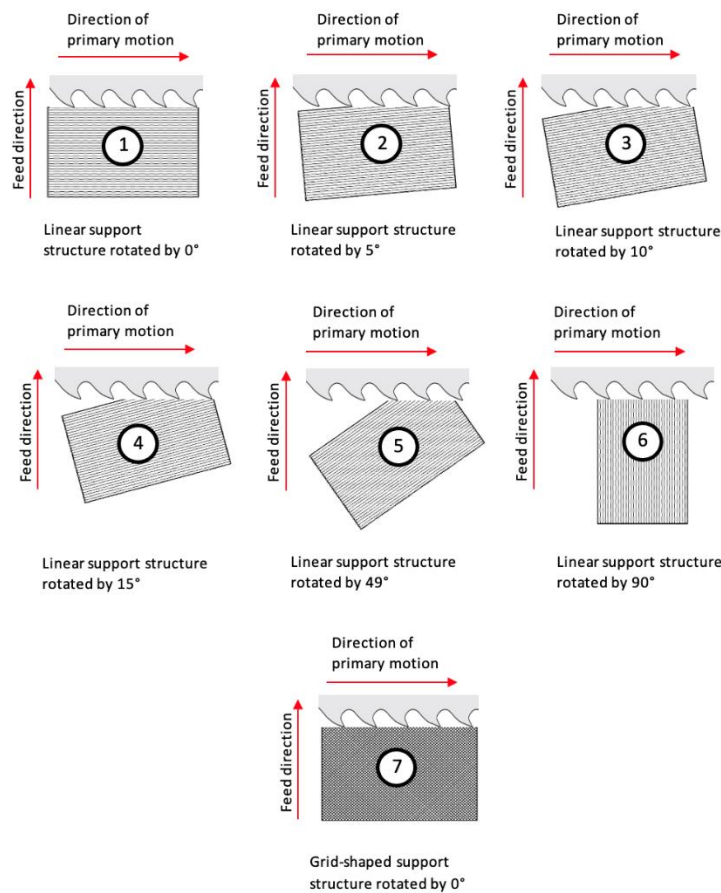

Fig. 2. Orientation of the LPBF cubes and their support structure on the substrate plate. 1-6: linear support structure, 7: grid-shaped support structure

Depending on the position of the cubes or their structural orientation on the substrate plate, different pressure angles were realized in relation to the direction of primary motion in the sawing process: 0° (cubes 1 and 7), 5° (cube 2), 10° (cube 3), 15° (cube 4), 45° (cube 5), 90° (cube 6). Figure 2 shows schematically the contact conditions of the bandsawing process resulting from the orientations as well as the motion of primary cutting and the feed direction.

The Ti6Al4V test components were produced using a TruPrint 1000 AM system made by Trumpf [15]. The system is a laser metal fusion (LFM) 3D printer that builds components layer by layer (additively) by melting metal powder with a laser. The manufacturing process carried out by this system is called LPBF (laser powder bed fusion). The integrated laser of the 3D printer has a maximum laser power of 200 watts. The maximum volume that can be produced is a cylinder with a height of 100 mm and a diameter of 100 mm. The printing process was carried out in the absence of oxygen in an inert argon atmosphere to avoid oxidation processes. The printing process of the test component was carried out with the following parameter settings (Tables 1 and 2):

Table 1. Configuration settings.

Hatching offset	Hatching distance	Pattern
0.030 mm	0.11 mm	chequerboard

Table 2. Scan settings.

Parameters	Hatching	Edge contour
Laser beam diameter	0.030 mm	0.030 mm
Laser speed	1,200 mm/s	1,000 mm/s
Laser power	155 W	75 W

3. SAWING PROCESS

The cubes were separated from the substrate plate using a Kastowin amc band saw by Kasto, which was specifically developed for cutting operations in the area of additively manufactured components. For the sawing process, the base plate of the saw rotated by 180° in such a way that the components were cut off upside down and fell downwards into a collecting container [16]. The distance between the machine table and the LPBF substrate plate could be set individually between $12 - 50$ mm, depending on the height of the substrate plate. The band saw blade used had a dimension of $5,090 \times 34 \times 1.1$ mm.

In order to be able to determine the machining forces in the sawing process, a piezo-electric three-component force measuring platform of the type MiniDyn 9119AA1 by Kistler was mounted between the machine table and the substrate plate. The measuring platform can absorb forces up to a maximum of 4 kN in each of the three directions of x, y and z [17]. In addition, the sawing process was monitored with an acoustic emission system by Quass using a sensor of the type Optimiser4D and the measuring mode of high-frequency impulse measurement (HFIM). The system enables a time – and frequency-resolved evaluation of structure-borne sound signals during the saw cut [18]. The measuring set-up described is shown in Fig. 3.
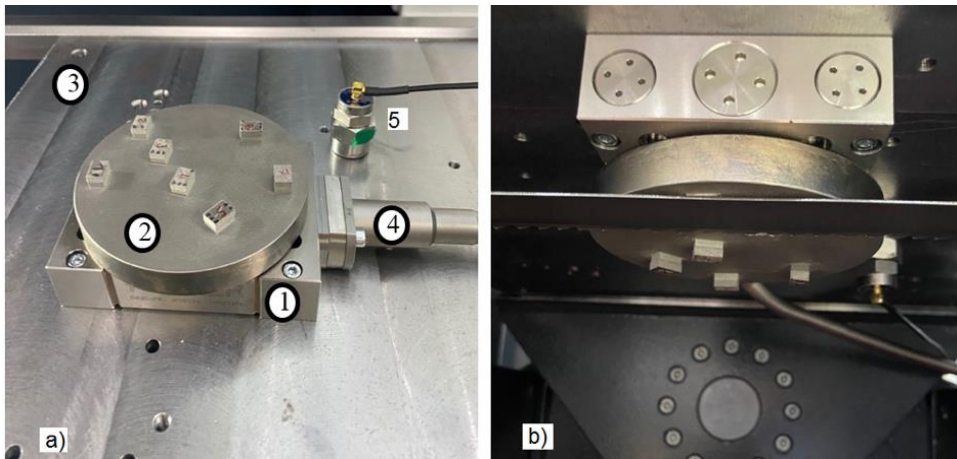
Fig. 3. a) Experimental setup force measurement: 1) measuring platform, 2) LPBF substrate plate, 3) machine bench, 4) 8-pole connection cable, 5) measuring sensor Optimizer4D; b) cutting process

4. TEST RESULTS AND DISCUSSION

The test cubes were cut off at a cutting speed of $v_c = 12.5$ m/min, a feed rate of $v_f = 25.4$ mm/min and a feed per tooth of $f_z = 0.015$ mm in a dry cut without using cutting fluid. The length of the saw band was $l_b = 5,090$ mm, the tooth pitch was $A = 7$ mm and the number of teeth was $Z_{Band} = 1,786$. The saw cut was guided only through the support structure. The distance between the saw blade and the surface of the substrate platform was 1 mm. The process was divided into seven individual steps in order to be able to determine the machining forces and vibrations for each cube separately.

4.1. INFLUENCE OF THE SUPPORT STRUCTURE ON THE PROCESS FORCES

Figures 5 to 8 show the course of the machining forces when sawing through the support structures of the cubes. The direction of primary motion runs not only parallel to but also perpendicular and at varying angles to the orientation of the elements in the linear support structure. This led to great fluctuations in machining forces during the sawing process. In comparison to cubes 1–5, significantly higher resultant forces were generated when sawing off cubes 6 and 7. This could be explained by the interrupted cut of the sawing process since the first tooth engagement. It was of interest to take a closer look at the sawing process and the declining resultant forces with regard to the orientation of the linear support structures to the direction of primary motion. For that purpose, the maximum length of the tooth engagement and the time required for this were calculated theoretically and extrapolated to the course of the forces determined by experiment. The maximum length of the tooth engagement l_{max} was reached at a depth of cut h_{min} and remained constant for some time until the depth of cut h_{max} was reached (Fig. 4). Both depths of cut h_{min} and h_{max} depended on the positioning of the support structure and could be calculated together with the length and time of engagement according to the following formulae (1–5).
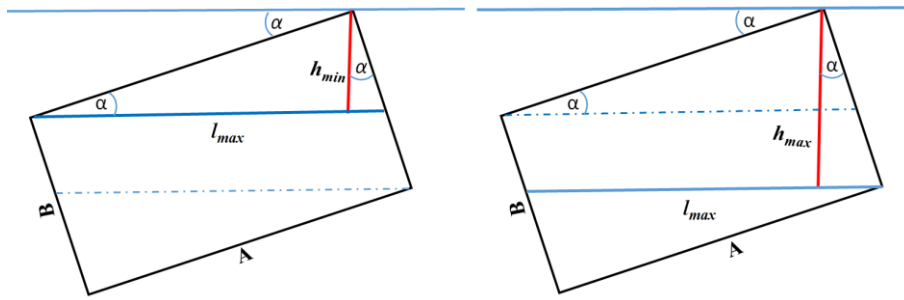
Fig. 4. Schematic representation of the length of the saw tooth engagement in the support structure.
A-length and B-width of the support beams

$$h_{min} = min(A * sin(\alpha), B * cos(\alpha)) \quad \alpha \neq 0, \quad \alpha \neq 90 \tag{1}$$

$$h_{max} = max(A * sin(\alpha), B * cos(\alpha)) \quad \alpha \neq 0, \quad \alpha \neq 90 \tag{2}$$

$$l = \begin{cases} \dfrac{2h}{sin(2\alpha)} & 0 \leq h \leq h_{min} \\ \dfrac{2h_{min}}{sin(2\alpha)} & h_{min} \leq h \leq h_{max} \end{cases} \quad \rightarrow \quad \rightarrow \quad \alpha \neq 0, \quad \alpha \neq 90 \tag{3}$$

$$l_{max} = \frac{2h_{min}}{sin(2\alpha)} \tag{4}$$

$$t_{min} = \frac{h_{min}}{v_f} \tag{5}$$

where: h – depth of cut, h_{min} – minimum depth of cut at maximum length of engagement, h_{max} – maximum depth of cut at maximum length of engagement, α – positioning of the support structure to the direction of primary motion, l_{max} – maximum length of engagement, t_{min} – time to reach the minimum depth of cut h_{min}, v_f – feed rate.

Table 3 shows the calculated depth of cut and time when the length of the saw engagement in the support structure reaches its maximum. Cube 1 (0°) reached the maximum length of engagement with l_{max} = 10 mm already within the first tooth pass. Regarding cube 6 (90°), the tooth passed 33 beams of the support structure. The total length of cut was 6.5 mm, including a 3.3 mm length of beam contact.

Because the length of the saw tooth engagement increased from the beginning of the sawing process t_0 up to the calculated t_{min}, this period of time was applied to the course of the machining forces and analysed. Cube 1 had an average cutting force of F_c = 65 N and an average feed force of F_f = 30 N after 48–55 ms (Fig. 5a). For cubes 2–5, a proportional increase in cutting and feed force could be seen between t_0 and t_{min} (Fig. 5b, Fig. 6 and Fig. 7).

Table 3. Depth of cut, length of engagement and time for sawing the support structure

α	h_{min} [mm]	h_{max} [mm]	l_{max} [mm]	t_{min} [s]	t_{max} [s]
0° (Cube 1)	-	7.000	10.000	-	17.647
5° (Cube 2)	0.872	6.973	10.020	2.055	17.571
10° (Cube 3)	1.736	6.893	10.174	4.110	17.369
15° (Cube 4)	2.588	6.761	10.360	6.118	17.042
45° (Cube 5)	4.949	7.071	9.900	11.692	17.823
90° (Cube 6)	-	10.000	3.300	-	25.210

This effect was limited to sawing with a continuous cut (cubes 1–5). For cube 5 (45°), the lowest value of $l_{max} = 9.9$ mm and the maximum value of $t_{min} = 11.692$ mm were calculated. When t_{min} was projected onto the force curve (Fig. 7), a slow constant increase in cutting force F_c from 0 to 108 N and in feed force F_f from 0 to 87 N could be seen. Compared to cubes 1–4, these forces were approximately 10–40 N (F_c) and 30–50 N (F_f) higher. This could be attributed to the temperature rise in the component with growing time/depth of cut.
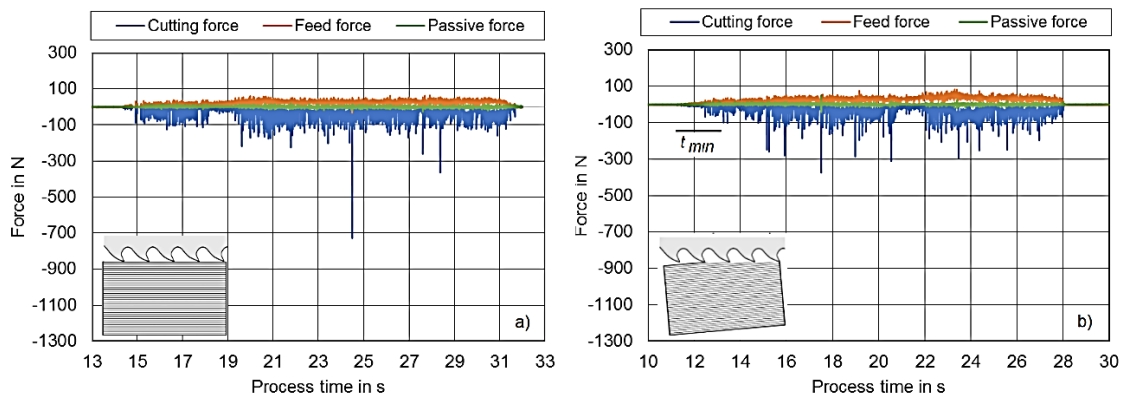
Fig. 5. Forces during sawing: Cube 1 (a): linear support structure, the position of the support structure to the direction of primary motion: 0°; Cube 2 (b): linear support structure, the position of the support structure to the direction of primary motion: 5°

According to the theoretical analysis, l_{max} should be constant for a depth of cut between h_{min} and h_{max} (t_{min} -t_{max}) and should decrease after reaching h_{max} (t_{max}) (Fig. 4). It was to be expected that the resultant forces would also decrease correspondingly after the time of t_{max} (Table 3). This assumption could not be found because the test components were not completely sawn off. The final separation of the cubes from the substrate plate occurred by breaking off the remaining support structures (see Chapter 4.3 below).

Sawing the linear support structure with interrupted cut (cube 6) led to a more unstable sawing process and caused an increase in resultant forces of approximately 10–20 percent compared to cubes 1–5 (Fig. 8a).
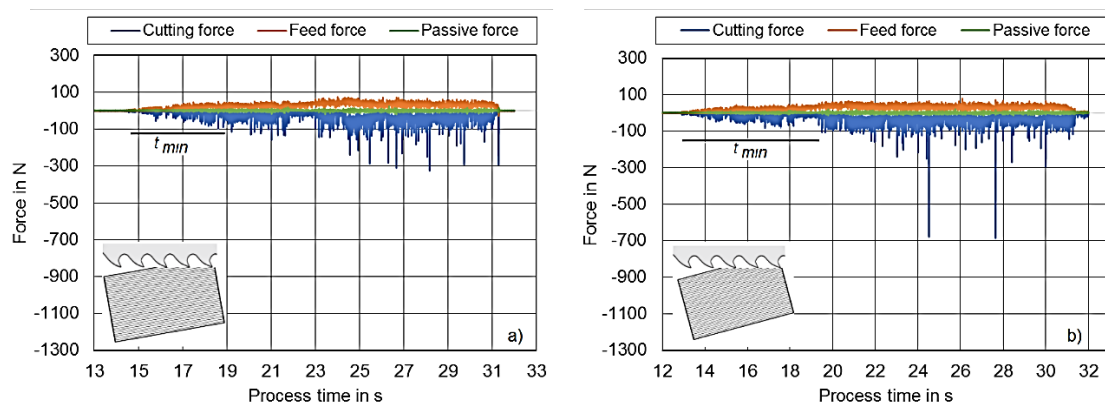
Fig. 6. Forces during sawing: Cube 3 (a): linear support structure, the position of the support structure to the direction of primary motion: 10°; Cube 4 (b): linear support structure, the position of the support structure to the direction of primary motion: 15°

Regarding the sawing through a grid-shaped support structure (cube 7), the cutting force as well as the feed force reached the highest determined values of $F_c = 140$ N and $F_f = 95$ N (Fig. 8b). This could be explained by the higher volume of the grid structure of 198 mm² and the interrupted cut.
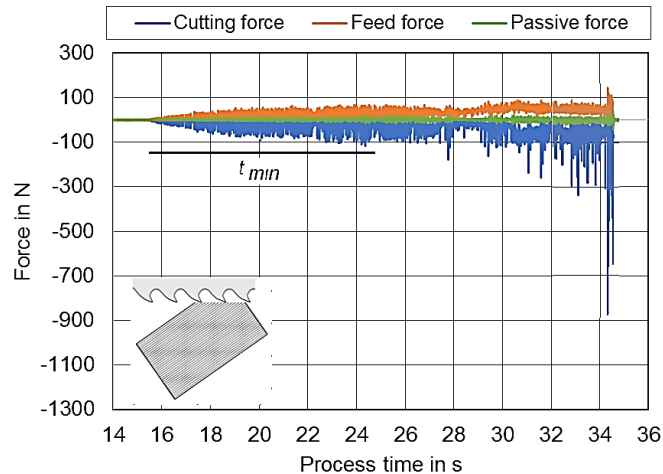

Fig. 7. Forces during sawing: Cube 5: linear support structure, the position of the support structure to the direction of primary motion: 45°

All in all, a greater increase in resultant forces was observed when sawing the support structure with an interrupted cut from the beginning of the process. This could be explained by the increasing material removal rate under more and more difficult conditions of chip removal.
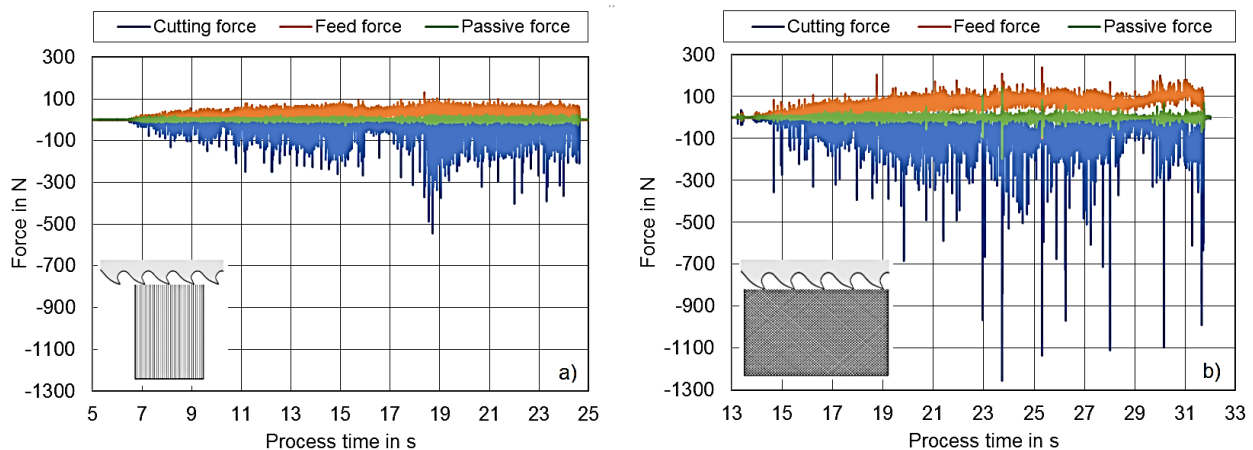

Fig. 8. Forces during sawing: Cube 6 (a): linear support structure, the position of the support structure to the direction of primary motion: 90°; Cube 7: grid-shaped support structure, the position of the support structure to the direction of primary motion: 0°

It should be noted that there was a decrease in forces approximately between 1.7–1.8 s in all curves of the sawing process. This was a result of the abrasively worn-out tooth tips of the bandsaw, which could not engage at a feed rate of $v_f = 25.4$ mm/min. For that reason, the material removal volume increased for the next teeth, resulting in a significant increase in

cutting and feed forces. In addition, many more regular/irregular increases in force could be seen in the cutting force curves. It could be assumed that these increases were due to the adhesive wear of some teeth. The unstable sawing process caused the local inhomogeneities of the cut surface and led to the decrease in flatness of sawn support structure areas.

4.2. VIBRATIONS DURING SAWING OF THE SUPPORT STRUCTURES

The sawing process was monitored with the acoustic emission system described above, which was positioned on the base plate of the band saw (200 mm behind the substrate plate). The sensor enabled a time- and frequency-resolved evaluation of structure-borne sound signals during the sawing off of the test cubes from the support plate. The signals were analysed using the Fourier transformation (FFT) and presented in the form of FFT cascade diagrams (Fig. 9 and Fig. 10).

In the evaluation of the structure-borne sound signals obtained when sawing off the cubes with a linear support structure (cubes 1, 2, 3, 4), only slight differences between the respecttive cascade diagrams could be detected. In contrast, there were clear differences between the structure-borne sound signals when sawing off the cubes 1, 5, 6 and 7, which were therefore considered in particular.

Figure 9 shows the FFT cascade diagrams of the process frequencies for cube 1 and 5. In both diagrams, there are low frequencies of $f = 4$–5 kHz before the first tooth engagement in the support structure. These frequencies can be attributed to natural frequencies of the idling process and occur also after the saw band exit and during the entire sawing process, yet at comparatively higher signal amplitudes. Other significant frequencies are in the ranges of 10–20 kHz, 50–70 kHz, 125–140 kHz, 190–210 kHz and 240 kHz. Although the frequency ranges are essentially the same for both sawing processes, the respective signal amplitudes differ. In cube 1, for example, the signal amplitudes are relatively uniform for all 3 frequency ranges. In cube 5, however, the signal amplitudes are significantly higher and, above all, abruptly changing after half of the machining time. This indicated a greater instability of the sawing process when the support structure of the LPBF component is positioned at a 45° angle against the direction of primary motion.
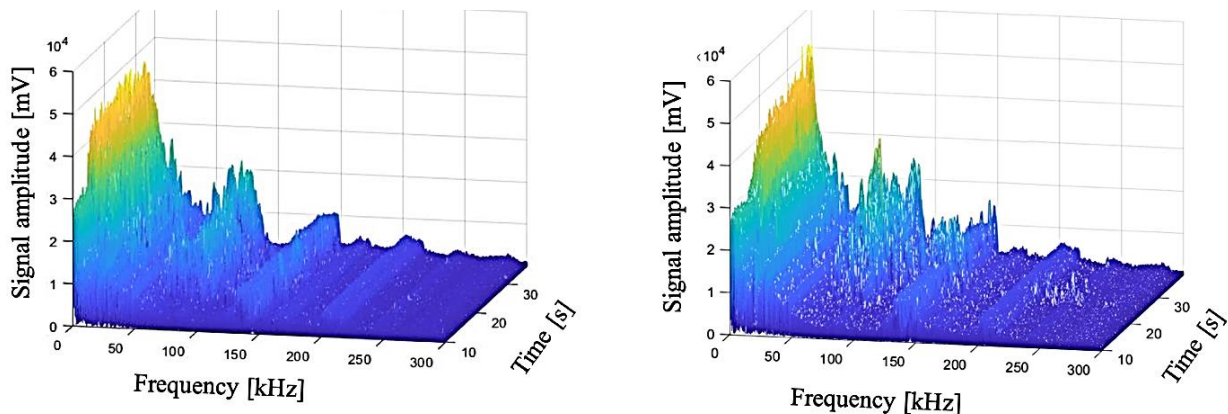

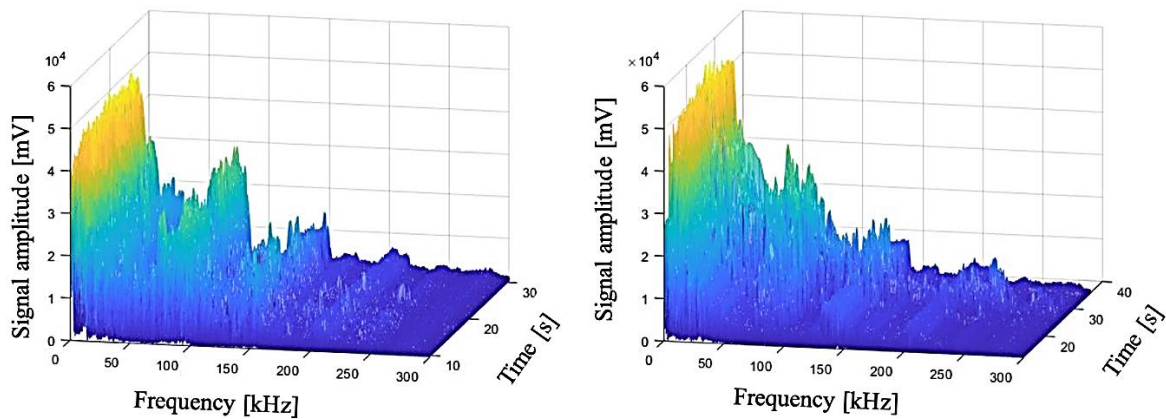Fig. 9. FFT cascade diagrams of the process frequencies for cube 1(a) and cube 5 (b)

Fig. 10. FFT cascade diagrams of the process frequencies for cube 6(a) and cube 7 (b)

Figure 10 shows the FFT cascade diagrams for cubes 6 and 7. Compared to cubes 1 and 5, even higher signal amplitudes were determined for both cubes in the frequency range between $f = 70–140$ kHz. It could be seen that the grid-shaped support structure of cube 7 was the only one with a high signal amplitude of more than 5×10^4 mV. In the case of a perpendicular arrangement of the linear support structure (cube 6) and the resulting interrupted cut, signal peaks in the range of up to 150 kHz were clearly more frequent than in comparison to all other cubes with a linear support structure.

It can be concluded that the support structures which were predominantly sawed off in an interrupted cut were subject to an increased process instability. For the thin-walled LPBF components, the linear support structures can therefore be preferred. The linear support structures of the LPBF components should be positioned at a 0–15° angle against the direction of the primary motion of the saw blade.

4.3. QUALITY OF THE BANDSAWING PROCESS

Looking at the LPBF cubes after the sawing process revealed that the support structure was not completely sawn off for any of the cubes. The remaining support elements (cubes 1–7, Fig. 11) indicated that the cubes were finally teared off from the substrate platform. Due to their thin walls, it is possible to manually remove the remaining linear support structures of cubes 1–4.

Regarding cube 5 (45° angle to the direction of primary motion), the support structure remained in an area corresponding to approximately 50% of the area to be cut (Fig. 11.). The support structure was sawn only in the first 6 s of the sawing process. Afterwards, the support beams were partly sawn, partly torn off, but not separated from the support platform. This was reflected in an increase in the resultant forces of the sawing process (Fig. 7), as the material volume to be machined became larger and larger due to the remaining structure. Before the cube was torn off, the resultant forces reached a maximum value of $F_c \geq 800$ N and $F_f \geq 150$ N. Removing the more massive support structure from cube 5 required significantly more effort compared with the individual support beams of cubes 1–4. Approximately 70% of the support structure of cube 6 was cut off from the cube surface. Out

of 33 support beams, eleven beams were completely sawn off and five beams were partially sawed off. The remaining 17 beams were partially or completely torn off the support platform.

The support structure adhering to cube 7 melted away due to the grid-shaped arrangement and the high mechanical load during the sawing process. Figure 11 shows the separation surface with the fused support structure as well as the remaining fused support grids. Due to the higher density of the fused structure, more effort was necessary to remove it from the cube. It is recommended to remove the support structure adhering to the cubes 5, 6 and 7 by machine.
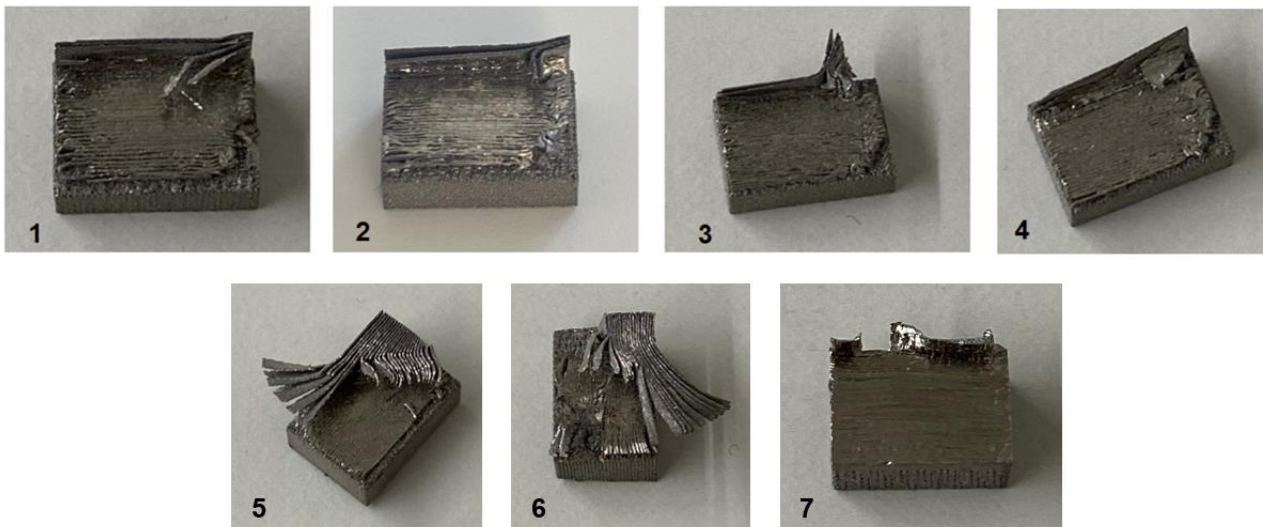

Fig. 11. Support structure after sawing off. Cube 1-6: linear support structure (0°, 5°, 10°, 15°, 45° and 90°), Cube 7: Grid-shaped support structure (0°)

Compared to manual removal, machine finishing is much more time-consuming and costly. In addition, the risk of damaging the component increases during machining. For the thin-walled LPBF components, the linear support structure should therefore be preferred with regard to the removal of the support structures. During the sawing process, the support structure should be positioned at a small angle of <15° to the direction of primary motion. It should be noted that the machine finishing process cannot be avoided for components with great demands on the surface quality of the cut area.

5. CONCLUSION

The investigations carried out showed a strong influence of the support structure on the separation of the LPBF test components from the substrate plate by means of the bandsawing process. It was found out that the arrangement on the substrate plate as well as the material volume of the support structure had a great influence on the process forces and vibrations acting on the component. The lowest forces and thus the lowest mechanical load on the component was achieved by a linear support structure arranged parallel to the direction of primary motion. In contrast, the grid-shaped support structure generated significantly

higher mechanical loads due to the higher material volume and the interrupted cut. This is of great importance when sawing off thin-walled LPBF components, in order to avoid high mechanical loads and vibrations as far as possible. In future investigations, the process forces during the sawing of LPBF components will be further reduced. For that purpose, the use of cutting fluid in the sawing process and the process parameters will be optimized. In addition, band saw blades with different/variable tooth angles will be used and tested.

ACKNOWLEDGEMENTS

REFERENCES

[1] DILBEROGLU U.M., GHAREHPAPAGH B., YAMAN U., DOLEN M., 2018, *The Role of Additive Manufacturing in the Era of Industry 4.0,* Procedia Manufacturing, 11, 545–554.

[2] THOMPSON M.K., MORONI G., VANEKER T., FADEL G., CAMPBELL R.I., GIBSON I., BERNARD A., SCHULZ J., GRAF P., AHUJA B., MARTINA F., 2016, *Design for Additive Manufacturing: Trends, Opportunities, Considerations, and Constraints*, CIRP Annals, 65/2, 737–760.

[3] KARAKURT I., LIN L., 2020, *3D Printing Technologies: Techniques, Materials, and Post-Processing*, Current Opinion in Chemical Engineering, 28, 134–143.

[4] DEBROY T., WEI H.L., ZUBACK J.S., MUKHERJEE T., ELMER J.W., MILEWSKI J.O., BEESE A.M., WILSON-HEID A., DE A., ZHANG W., 2018, *Additive Manufacturing of Metallic Components – Process, Structure and Properties*, Progress in Materials Science, 92, 112–224.

[5] AVRAMPOS P., VOSNIAKOS G.C., 2022, *A Review of Powder Deposition in Additive Manufacturing by Powder Bed Fusion,* Journal of Manufacturing Processes, 74, 332–352.

[6] WISCHEROPP T.M., 2021, *Advancement of Selective Laser Melting by Laser Beam Shaping*, Springer Vieweg, Berlin.

[7] KRANZ J., HERZOG D., EMMELMANN C., 2015, *Design Guidelines for Laser Additive Manufacturing of Lightweight Struktures in Tial6v4*, Journal of Laser Application, 27, S14001.

[8] BHUVANESH KUMAR M., SATHIYA P., 2021, *Methods and Materials for Additive Manufacturing: a Critical Review on Advancements and Challenges*, Thin-Walled Structures, 159, 107228.

[9] ISAEV A., GRECHISHNIKOV V., PIVKIN P., KOZOCHKIN M., ILYUHIN Y., VOROTNIKOV A., 2016, *Machining of Thin-Walled Parts Produced by Additive Manufacturing Technologies,* Procedia CIRP, 41, 1023–1026.

[10] MÖHRING H., BECKER D., MAUCHER C., 2022, *Spanntechnik beim Absägen von AM-Bauteilen*, wt Werkstatttechnik online, 112, 61–66.

[11] DENKENA B., DITTRICH M.A., HENNING S., LINDECKE P., 2018, *Investigations on a Standardized Process Chain and Support Structure Related Rework Procedures of SLM Manufactured Components,* Procedia Manufacturing, 18, 50–57.

[12] HINTZE W., WENSERSKI R., JUNGHANS S., MÖLLER C., 2020, *Finish Machining of Ti6Al4V SLM Components Under Consideration of Thin Walls and Support Structure Removal,* Procedia Manufacturing, 48, 485–491.

[13] MAUCHER C., MÖHRING H.-C., 2020, *Optimized Support Structures for Postprocessing of Additively Manufactured Parts,* MIC Procedia, 20, 141–146.

[14] MAUCHER C., TEICH H., MÖHRING H.-C., 2021, I*mproving Machinability of Additively Manufactured Components with Selectively Weakened Material,* Prod. Eng. Res. Devel, 15, 535.

[15] https://www.trumpf.com/de_DE/produkte/maschinen-systeme/additive-fertigungssysteme/truprint-1000.

[16] https://www.kasto.com/en/saws/bandsaws/bandsawing-machines-detail/kastowin-amc.html.

[17] https://www.kistler.com/files/document/003-055d.pdf.

[18] https://www.qass.net/wp/produkte/optimizer4d/.